



# Geometrical optimization of bumper beam profile made of pultruded composite by numerical simulation



Giovanni Belingardi, Alem Tekalign Beyene\*, Ermias Gebrekidan Koricho

Politecnico di Torino, Department of Mechanical and Aerospace Engineering, Corso Duca degli Abruzzi, 24, 10129 Torino, Italy<sup>1</sup>

## ARTICLE INFO

### Article history:

Available online 7 March 2013

### Keywords:

Bumper beam  
Optimization  
Pultruded  
Composite structures  
Geometrical profile  
Crashworthiness

## ABSTRACT

In addition to their high specific strength and specific stiffness composite materials possess high energy absorption capability, that makes them an interesting alternative material for developing automotive safety component, when to combine weight saving and crashworthiness is highly desirable.

In this work E-Glass/epoxy pultruded bumper beam is considered and its energy absorption capability is compared with steel and E-Glass/epoxy fabric composite. Furthermore, low velocity impact finite element simulations are performed using ABAQUS, in order to optimize beam section profile and beam curvature for crashworthiness. Results show that, pultruded bumper beam has comparable energy absorption capability with respect to the steel normal production solution. The new composite solution, after appropriate optimization of bumper beam section profile and beam curvature, exhibits yields improved energy absorption characteristics; the development of progressive failure mode leads to lower mean crash load and almost constant force diagram whose value is close to the maximum peak load.

© 2013 Elsevier Ltd. All rights reserved.

## 1. Introduction

Automobile bumper subsystem is the frontal and rear structure of the vehicle that has the purpose of energy absorption during low velocity impact. Usually, bumper subsystem consists of bumper transverse beam, stays, impact-absorbing materials in the form of structural components and a cover. Among those elements, the bumper beam is the main structural component; it is expected to be deformable enough to absorb the impact energy, in order to reduce the risks of injury for pedestrians and other vulnerable road users, but, at the same time, it should also have sufficient strength to protect the nearby vehicle components. Therefore, during bumper beam design process the challenging task is to obtain the optimal characteristics, since there is a tradeoff between strength and deformability.

Due to their enhanced physical and mechanical properties, such as high specific strength, both in static and impact loading conditions, and high specific stiffness (light weightiness), composite materials could be an interesting candidate material for this component. When designing with composite material, it is always needed to select the type of production technology that will be used in manufacturing, as this choice will affect deeply both the cost and the production rate. As a matter of fact, up to now, in spite

of composite attractive mechanical features, their relatively low volume of production and high material cost have hindered their intensive application for automotive structural components [1].

Pultrusion is a rapidly growing, cost-effective and fully automated manufacturing process for producing constant cross-section composite profiles. Generally, pultruded profiles have straight axis, however some recent experience [2] shows that profiles with curved axis could also be produced with this manufacturing techniques. For the structural component of interest, pultrusion could be an appropriate composite manufacturing technology able to obtain high production rate with reasonable low manufacturing cost. Besides, pultruded products have very high quality in terms of geometry accuracy and degree of consistency of mechanical property due to process automation, they have also quite high compression strength, due to precise filament alignment and high fiber volume fraction (up 85% by weight) [1,3], as a consequence of material curing under tension.

Nowadays, pultruded composite products have become widely used in structural engineering applications and have been selected for some road components like roadside safety structures [4] and vehicles safety components such as bumper and crush box [4–6], where these structures are submitted to impact loading conditions.

Published experimental studies [7,8] show that pultruded composites (PFRP) have comparable and sometimes even higher values of energy absorption capability and impact force resistance with respect to steel and aluminum. The impact responses and damage mechanisms for the whole group of composite materials is relatively more complex than conventional materials and it depends

\* Corresponding author. Tel.: +39 3490828957.

E-mail addresses: [giovanni.belingardi@polito.it](mailto:giovanni.belingardi@polito.it) (G. Belingardi), [alem.beyene@polito.it](mailto:alem.beyene@polito.it) (A.T. Beyene), [ermias.koricho@polito.it](mailto:ermias.koricho@polito.it) (E.G. Koricho).

<sup>1</sup> <http://www.polito.it>.

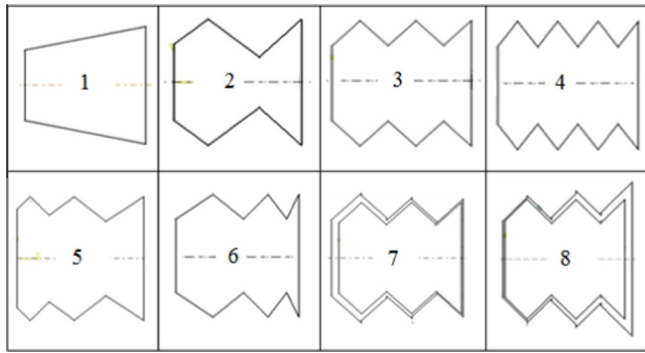


Fig. 1. Bumper beam profiles considered.

on a number of different parameters including fiber and matrix type, section shape and dimensions, impact velocity, impact angle, shape of striker, target geometry and target material [7]. In addition, although material characterization study, performed with coupons cut from pultruded tubes wall, does not put in evidence ductile material response, a pultruded tube is nevertheless capable of absorbing significant impact energy by behaving in a pseudo-ductile structural mode. This pseudo-ductile response in composite material tubes is obtained primarily from material fragmentation and large changes in the tubes cross-sectional geometry when the tube undergoes large flexural deformation [9].

When design is aimed to substitute existing metallic vehicle components with similar components made of new materials like composite, at first, it is important to take into account the different failure modes of the new material types as well as the system as a whole when it is submitted to dynamic impact loading. This is due to the fact that, crashworthiness in safety components is the fundamental characteristic and it mainly depends on the energy absorption mechanisms of the material and of the system. A second important point is that, generally, the component geometry has to be modified accordingly, so that the component can perform its intended use with the optimal capacity.

Published studies [4,9] show that, unlike metallic materials such as steel and aluminum, the energy absorption with composite material is not as a consequence of large plastic deformation but of progressive axial fracture for axially loaded components and of progressive tearing along the corner for transversally loaded components. The variables that control the energy absorption are the mechanical properties of fiber and matrix resin, fiber and resin volume fractions, laminate stacking sequence, fiber orientation and component geometry.

Energy absorption mechanisms for fiber-reinforced composite material tubes subjected to axial loading have been studied by a number of authors [5,6,10,11] and it is quite well understood that the energy absorption is due to the concurrence of different mechanisms such as wall delaminations, delamination penetration with

axial cracks formation and bending of petals followed by fiber fracture. These fiber fractures give place to fracture line formation across the tube wall. On the contrary, the energy absorption mechanisms for composite material tubes subjected to transverse loading, i.e. in bending and shear as it is the usual loading conditions for bumper beams, have not been extensively investigated and are not well understood. There are few published research results, which suggest that flexural loaded composite components, like beam, absorb energy by progressive tearing along the beam corner [4,9,12]. Therefore, while it is now rather well known how to design composite material tubes to develop a stable or controlled crushing response under axial impact loading, there is not enough and clear information regarding how to design a composite material tube for stable load-carrying capacity under flexural impact loading.

In the present work, a numerical study is conducted to explore the possibility of substituting the current metallic bumper beam with E-Glass/epoxy pultruded composites and its energy absorbing capability is compared with steel and E-Glass fabric composite. Furthermore structural optimization of the beam section profile and curvature is also developed to obtain a stable flexural failure of the composite bumper beam.

The analysis is done through the investigation of impact event characteristic data, such as force/time, force/deflection, energy/displacement and deflection/time curves.

## 2. Conceptual design of the beam section profile

As it is reported in many literature papers, the failure of a composite profile subjected to lateral or axial compressive loads occurs usually in a catastrophic manner, unless a progressive failure triggering mechanism is provided. In the case of axially loaded tubes, triggering mechanism is usually obtained by machining special geometry at one of the extremity edges of the profile. The trigger geometry originates a localized failure area as a result of stress concentration; afterwards, the local failure area is progressively extended [6,10]. In the case of a transversally loaded composite profile, it is not possible to introduce triggering mechanisms of that type.

In the case of transversally loaded composite beam, the stress concentration area, where the localized failure initiates, and the consequent mode of progressive failure is achieved by introducing longitudinal stress concentration zones, these zones are well defined by the profile corners. Therefore, by introducing a number of properly positioned stress concentration zones (longitudinal corners), it is expected to have a number of progressive tearing lines, and consequently progressive energy absorption. Furthermore, the proper positioning of these lines is expected to prevent catastrophic failure of the beam.

For the optimization of the beam section profile, eight different beam section profiles have been selected, as shown in Fig. 1. In particular, the profiles of the first row of Fig. 1 are characterized by an

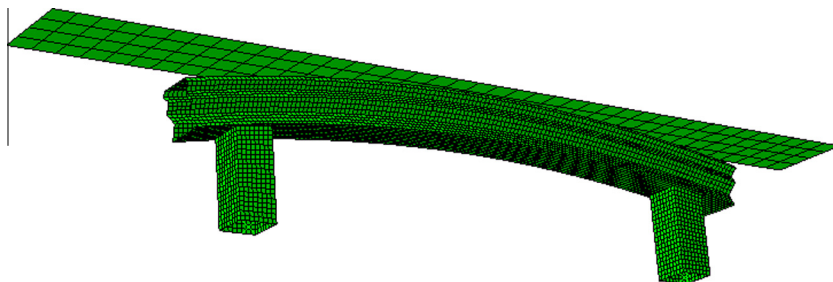


Fig. 2. FE model of simplified bumper beam.

**Table 1**  
True stress–plastic strain data for steel.

| $\sigma$ (MPa) | 304.6 | 344.19 | 385.51 | 424.88 | 450.39 | 470.28 |
|----------------|-------|--------|--------|--------|--------|--------|
| $\epsilon_p$   | 0     | 0.0244 | 0.0485 | 0.0951 | 0.1384 | 0.1910 |

increasing number of longitudinal grooves, while the second row shows some possible geometry variation of the profile 3.

The failure mode and energy absorption characteristics of all proposed section solutions are analyzed, while maintaining the same material properties, overall dimensions, loading and boundary conditions.

After having selected a section profile which exhibits the best crushing behavior, with a similar optimization procedure five different beam curvatures are analyzed.

During the optimization process of the beam section profile and curvature, changes in geometrical perimeters result in variation of load carrying capacity of the profile, but at the same time in variation of material amount i.e. mass. These two variations are not strictly correlated, although as a general trend [9] profiles having more material will be able to carry more load. Moreover results reported by S. Charoenphan et al. [4], indicate that an increment in the amount of material in the tubes gives an increment of the crack propagation rate. Therefore in present work, in order to identify the role of each geometrical parameter, by avoiding the eventual effect of mass changes, a constant amount of material is maintained through modifying the section profile by slight varying the wall thickness.

### 3. Numerical simulation and model description

By means of numerical simulations, it is possible to understand how the energy is distributed in the transverse beam structure with the progress of the deformation.

A nonlinear finite element simulation, with a simplified bumper beam model, as displayed in Fig. 2, is carried out using the commercial code ABAQUS/Explicit version 6.10-1. The model comprises four parts, three rigid parts, i.e. the two longitudinal crash boxes and one rigid wall, and one deformable transverse beam. The rigid bodies are modeled as discrete rigid surfaces in order to create higher mesh density at critical contact areas. The beam is made of E-Glass fiber–epoxy matrix pultruded composite material. A mass of 1000 kg is rigidly attached at the two rear extremities of the crash boxes, in order to simulate the vehicle mass, and is moving with an initial velocity of 15 km/h towards the rigid wall.

To evaluate bumper performance at low velocity impact, different organizations use different set of standards. For example, the Insurance Institute for Highway Safety (IIHS) suggests four test configurations, i.e. full width front and rear impacts against a flat barrier, a front impact against an angled barrier and a rear impact against a centered pole. All these tests are with an impact speed of 15 km/h except for the last test where the speed is reduced to 5 mi/h (about 8 km/h) (IIHS, 2002). The present study is not conducted to meet some specific standard and does not consider the entire bumper subsystem, but only the bumper beam. However, since the intention is to improve the energy absorption contribution of bumper beam in any impact circumstances through material substitution and section profile and beam curvature optimizations, the simulations have been conducted with relatively high impact velocity, i.e. 15 km/h.

**Table 2**  
Mechanical properties of E-Glass/epoxy pultruded and glass/epoxy fabric.

| Property  | $\rho$ (kg/m <sup>3</sup> ) | $E_{11}$ (GPa) | $E_{22}$ (GPa) | $G_{12}$ (GPa) | $G_{23}$ (GPa) | $\nu_{21}$ | Xc (MPa) | Xt (MPa) | Yc (MPa) | Yt (MPa) | Sc (MPa) |
|-----------|-----------------------------|----------------|----------------|----------------|----------------|------------|----------|----------|----------|----------|----------|
| Pultruded | 1850                        | 31.2           | 9.36           | 5              | 5.5            | 0.29       | 409      | 483      | 92.2     | 34.9     | 73.3     |
| Fabric    | 1850                        | 29.7           | 29.7           | 5.3            | 5.3            | 0.17       | 549      | 369      | 549      | 369      | 97       |

### 3.1. Material data

Three different materials are considered for this study:

- A mild steel with Young modulus  $E = 206$  GPa, Density  $\rho = 7830$  kg/m<sup>3</sup>, Poisson ratio  $\nu = 0.3$ , and true stress–plastic strain property as reported in Table 1.
- Two composite materials: a unidirectional pultruded and a bidirectional fabric E-Glass/epoxy, with mechanical properties as reported in Table 2.

### 4. Results and discussion

Three parameters, namely failure mode, displacement and load peak values, are considered for both material substitution study and beam geometries optimization.

The choice of the above proposed beam profiles (Fig. 1) is based on the hypothesis that, the increment of the number of stress concentration zones, i.e. folds in this particular case, helps for crack triggering mechanism and the variation of the beam profile by changing the length, depth and thickness of each groove are assumed to cause a mode of failure that has the desired characteristic of a propagating progressive failure along the beam axis direction.

When the bumper beam is subjected to frontal impact, concentrated stresses develop at the fold vertexes; points on the fold sides at equal distance from the impacted surface have the same stress levels. This is substantially equal in case of straight beam while a change in the beam curvature has an effect both on the stress distribution along the beam and on the stress values. So, with a properly designed beam profile, it is possible to get the desired energy absorption through controlled deformation. This also helps in reducing the peak load, which is one of the factors that has to be maintained under control during crash, since higher peak load leads to higher decelerations, and this may cause dangerous impacts and even injuries to the vehicle occupants.

#### 4.1. Section profile optimization

At first, profile optimization was conducted by increasing the number of folds, with the intention of helping the crack formation and ultimately leading to transverse progressive tear failure. The increment of number of folds considered in the analysis continued up to a number where the beam strength begins to decrease, as a consequence of a change in the failure mode. A limit has been reached, where folds are no more serving as intended. In this particular case, the limit is up to threefolds. As it is shown in Figs. 3 and 4: when the number of folds becomes three (profile number 4), the bumper beam impact behavior become unsatisfactory, particularly in Fig. 4 a high peak reaction force, that is three times higher than the remaining other three profiles, is detected. This implies that, at the chosen impact velocity, the energy cannot be completely absorbed by the beam and the crash boxes and other nearby components have to be involved in energy absorption process.

Comparing the results reported in Figs. 4 and 5 and Table 3 for the four considered profiles, it can be noted that, with comparable energy absorption, profile 3 shows a progressive failure mode, with minimum peak load. To achieve good energy absorption, the diagram of the bumper reaction force should be as much flat as

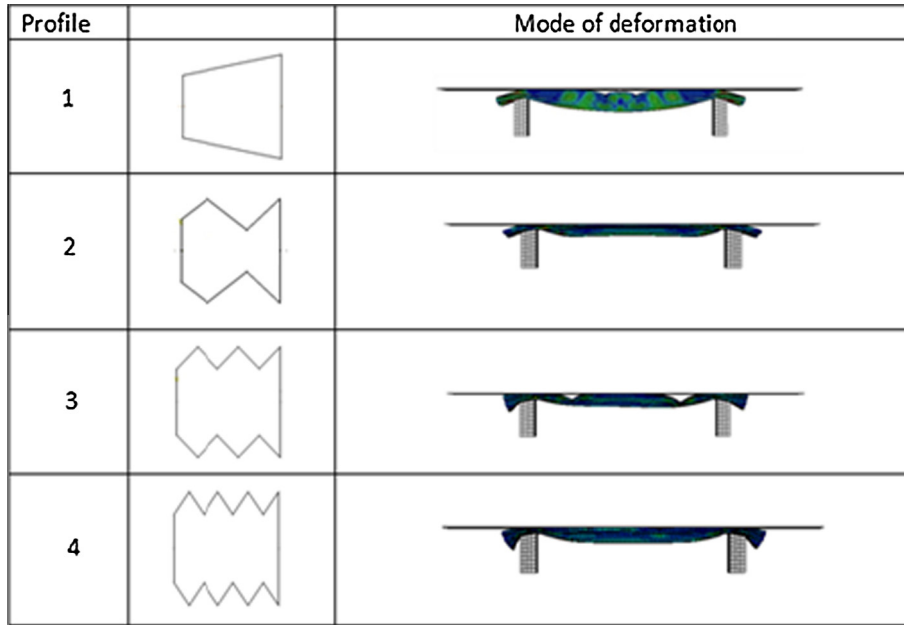


Fig. 3. Profile geometry and failure mode with different number of folds at 15 km/h impact velocity.

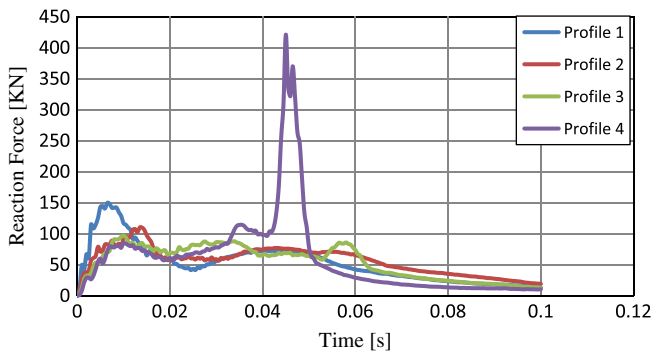


Fig. 4. Reaction force vs. time diagram of different number of folds with 15 km/h impact velocity.

Table 3  
Results of energy and peak loads for different profiles.

| Profile | Energy absorbed (kJ) | Peak load (kN) |
|---------|----------------------|----------------|
| 1       | 8.65                 | 149.98         |
| 2       | 8.70                 | 109.98         |
| 3       | 8.66                 | 96.73          |
| 4       | 8.67                 | 420.81         |

possible during the whole crash time and close to the maximum allowable level. With this regard, profile 3 has the mean load value that is close to the maximum peak load. Similarly, from energy vs. displacement curves of Fig. 5, it can be concluded that this profile has better linearity i.e. more progressive failure than the others.

Therefore profile 3 is selected as result of the first optimization step, and then a second step is done to further improve its performance through two different approaches. According to the first approach, profile 3 is modified by varying the fold width and depth so that the rear fold is deeper than the front one (profile 5); this leads to reduction in the profile strength when moving from the rigid wall toward crash box (as shown in Fig. 6). Its mode of failure and energy absorption has been compared with the reversed

profile geometry, profile 6, where the front fold is deeper than that of the rear one. As it is shown in Figs. 6 and 7, profile 5 gives an improved progressive failure whereas profile 6 experiences a local failure, a structure hinge comes out at the beam mid-span which results in a catastrophic fracture that leads to higher peak load and reduction in energy absorption with respect to profile 5.

According to the second approach, a similar progressive strength reduction is obtained by varying the wall thickness of each half of fold so that the wall thickness is greater at the front part of the profile and becomes progressively lower rearward, as shown in Fig. 8 (profile 7). Similarly, a comparison is made with reversed profile geometry. Analyzing the results reported in Figs. 8 and 9, it can be easily observed that profile 8 shows a local failure, due to the formation of structural hinge at the beam mid-span, which results in a catastrophic fracture that leads higher peak load and reduction in energy absorption with respect to profile 7.

Profiles 7 and 8 have a similar trend of failure mode with respect to the previously considered profiles 5 and 6, i.e. when the bumper transverse beam impacts at its weaker side; its failure mode becomes unstable and catastrophic. On the other hand, when the bumper transverse beam impacts against the rigid wall at its stronger side, a progressive failure is obtained.

A comparison of crash performance of profiles 5 and 7 can now be done with profile 3, which is the optimal result from the first

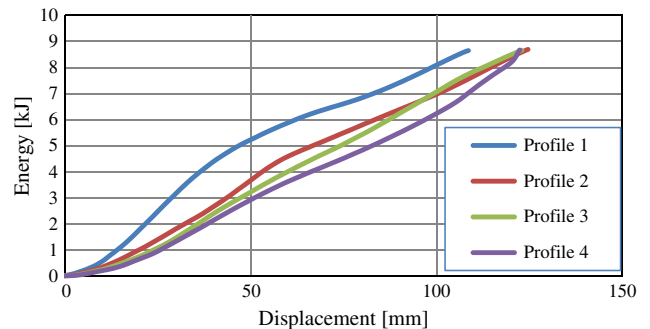


Fig. 5. Energy vs. displacement diagram of different number of folds with 15 km/h impact velocity.

| Profile |  | Mode of deformation |
|---------|--|---------------------|
| 5       |  |                     |
| 6       |  |                     |

Fig. 6. Profile geometry and failure mode varying fold width and depth along the beam high.

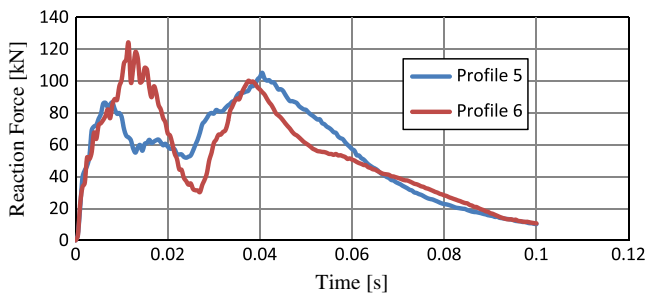


Fig. 7. Reaction force vs. time plot with varying fold length and depth with 15 km/h impact velocity.

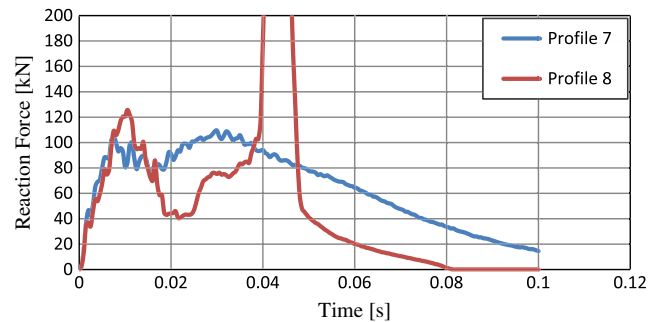


Fig. 9. Reaction force vs. time plot with varying wall thickness at 15 km/h impact velocity.

optimization step. It can be notice that, by means of these further geometry modifications, it is possible to improve both the mode of failure, i.e. failure progressivity, and the total energy absorption, in particular with profile 7, as clearly shown in Figs. 10–12 and in Table 4, although with a small increment of peak load.

#### 4.2. Beam curvature optimization

The third optimization step is devoted to the beam curvature. Using profile 7, which gives better energy absorption and mode of failure, out of the three, a further geometry optimization is conducted through varying the beam curvature. As mentioned before, five beam curvature, i.e. beam curvature radius of 2400, 2862, 3200, 3600 mm and straight beam are considered, and a investigation of impact event characteristic data are done with a procedure

similar to the one adopted in the previous paragraphs. Maximum peak load values and energy absorption results are presented in Table 5 for all profiles.

As a first general observation, when the beam curvature is increased, the formation of local stress concentration is reduced. This is due to the fact that larger zones of the bumper beam are in contact with the flat rigid wall at the same time. This leads to higher peak load that promote the formation of diffuse fractures on the portions of the folds which have the same stress level.

The worst case is when the bumper beam is straight, which is currently used by some vehicles. In this situation the portion of the beam extremities just in front of the crash box, with length equal to the crash box width will fracture at the same time, since

| Profile |  | Mode of deformation |
|---------|--|---------------------|
| 7       |  |                     |
| 8       |  |                     |

Fig. 8. Profile geometry and failure mode varying wall thickness along the beam section.

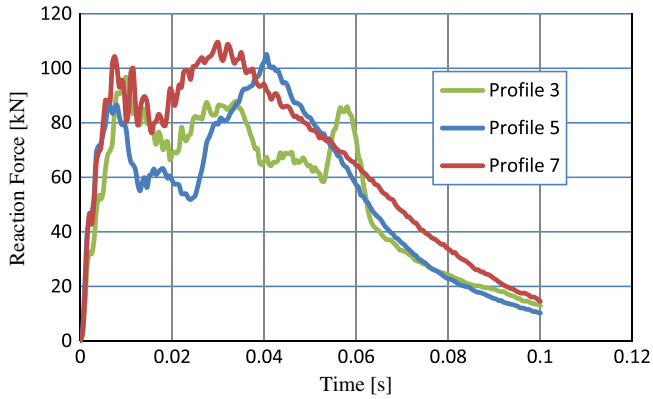


Fig. 10. Reaction force vs. time plot for three profiles at 15 km/h impact velocity.

Table 4  
Results of energy and peak loads value.

| Profile | Energy absorption (kJ) | Peak load (kN) |
|---------|------------------------|----------------|
| 3       | 8.663                  | 96.7           |
| 5       | 8.648                  | 105.1          |
| 7       | 9.852                  | 109.4          |

Table 5  
Results of energy and peak loads value.

| Radius (mm) | Energy absorption (kJ) | Peak load (kN) |
|-------------|------------------------|----------------|
| 2400        | 8.000                  | 276.7          |
| 2862        | 9.852                  | 109.4          |
| 3400        | 9.8585                 | 156.6          |
| 3600        | 9.8491                 | 381.1          |
| Straight    | 9.852                  | 1389.53        |

that portion of the beam is under equal stress level and there is not possibility for crack propagation and proper energy absorption. Therefore, for this type of structural profile and loading condition,

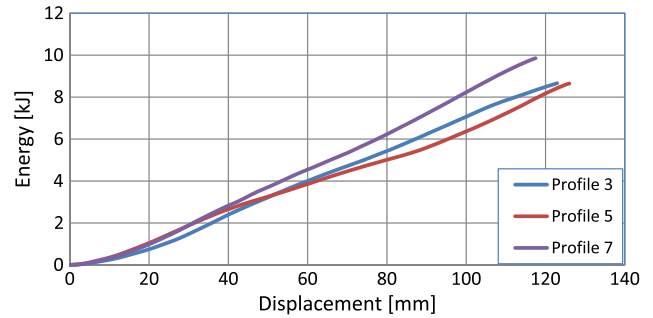


Fig. 12. Energy vs. displacement diagram for profiles 3, 5 and 7 at 15 km/h impact velocity.

inappropriate replacement of the existing steel beam with composite beam may cause a catastrophic failure.

On the other side, when the beam curvature is reduced below some critical curvature radius, 2862 mm in this particular case, there will not be time for crack propagation, instead a high local stress line will be developed at the apical portion of the beam, which resulted unstable failure as shown Fig. 13a. Therefore, in the case of straight beam (zero curvature), the contact between the rigid modeled crash boxes and the rigid barrier gives the maximum reaction force, as indicated in Table 5, while for the case of the smallest radius of curvature, local structural hinge at the beam mid-span gives place to unstable failure which leads a reduction of the energy absorption and even possible damage of the nearby components.

By observing reaction force vs. time curves in Fig. 14, it can be concluded that, the reduction of the bumper curvature radius gives a significant reduction of peak load value. Moreover, as it is shown in energy vs. displacement curves of Fig. 15, when beam curvature radius is increased or decrease beyond some critical value, the curve begins quite early to deviate from linearity i.e. the progressivity of the failure mode is not maintained. Generally, in design development of composite bumper beam, an optimal bumper beam curvature radius, besides improving vehicle aerodynamic performance, actually gives a contribution to the vehicle safety enhancement.

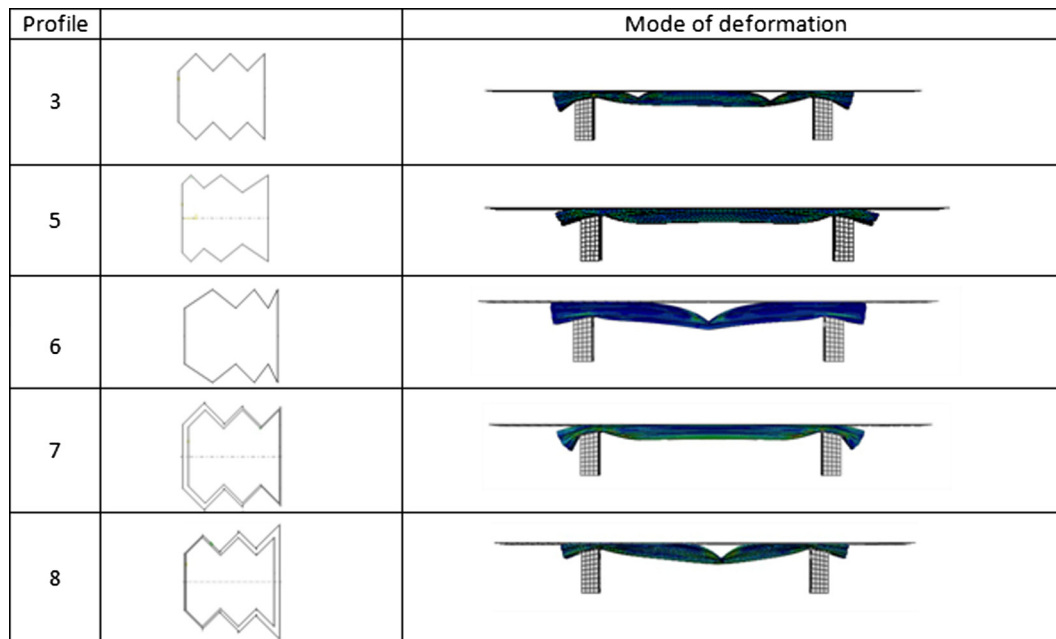


Fig. 11. Profile geometry and failure mode of profiles 3, 5 and 7.

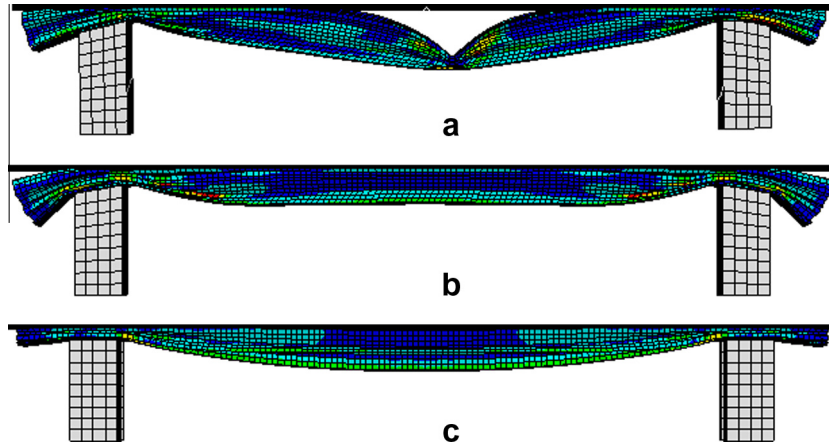


Fig. 13. Failure mode for curvatures of radius (a) 2400 mm, (b) 3200 mm, and (c) straight.

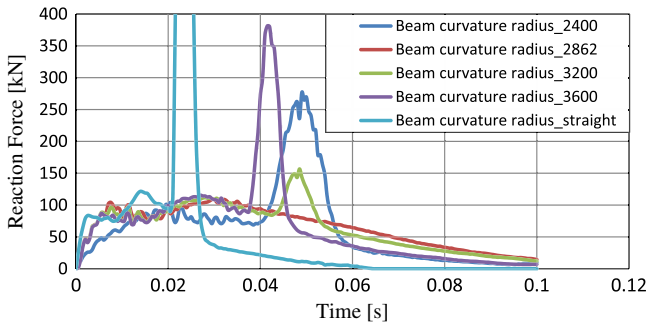


Fig. 14. Reaction force vs. time diagram for different beam curvatures.

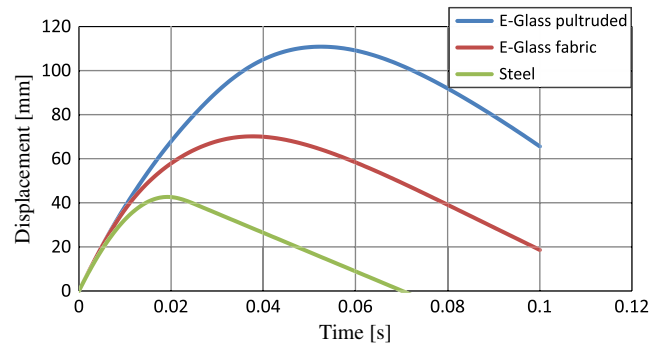


Fig. 16. Displacement vs. time for the three different material solutions.

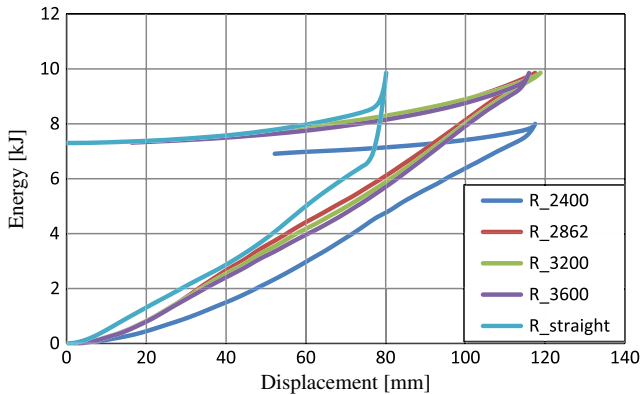


Fig. 15. Energy vs. displacement diagram for different beam curvatures.

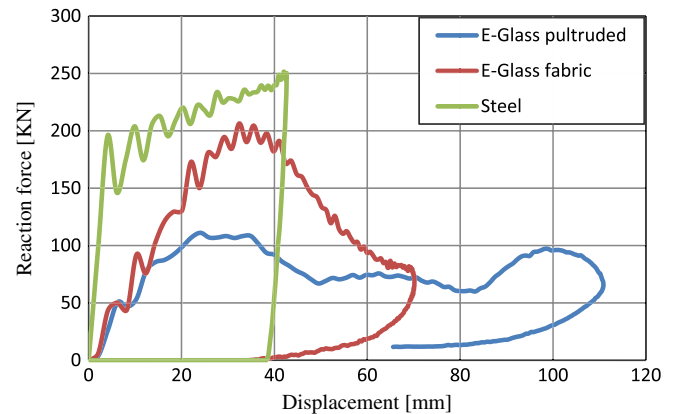


Fig. 17. Reaction force vs. displacement for the three different material solutions.

At the end of these three step optimization procedure the chosen solution for the E-Glass/epoxy pultruded composite beam is characterized by the section profile 7 and a beam curvature radius of 3200 mm, although other design details could lead to slight modifications of the beam performance. For this particular case, the chosen solution is the best option with a small cost in peak load with respect to the 2862 mm curvature radius beam but with safer margins for energy absorption.

#### 4.3. Comparison with other material solutions

Having identified the best profile with optimal values from above listed conceptual beam section profiles and curvatures,

based on the above mentioned energy absorption and failure pattern criteria, a pultruded composite bumper beam is proposed in the present study of material substitution, aimed to develop a vehicle with a lighter bumper beam.

It is now of interest to compare the obtained pultruded composite bumper beam solution with steel and glass fabric/epoxy composite solutions in terms of impact energy absorption and weight.

For this scope, two further simulations have been run, by keeping the entire geometrical and loading parameters constant except the material parameters.

**Table 6**  
Results of energy and peak loads.

| Material  | Energy absorption (kJ) | Peak load (kN) |
|-----------|------------------------|----------------|
| Steel     | 8.69                   | 251.56         |
| Fabric    | 8.67                   | 206.36         |
| Pultruded | 8.66                   | 109.4          |

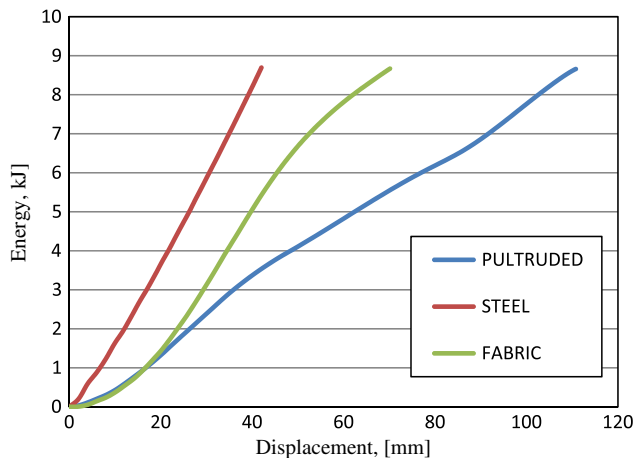


**Fig. 18.** Energy vs. displacement for the three different material solutions.

Figs. 16–18 show the curves of displacement vs. time, reaction force vs. displacement and energy vs. displacement curves, respectively. Numerical results are also reported in Table 6. All the three solutions absorb the same impact energy but the way the energy is absorbed, i.e. the failure mode, is completely different from each other. In addition the resulting reaction forces vary significantly.

As it is well known, the current trend in vehicle passive safety component design is to develop a frontal and rear crumpling zone that can absorb most of the impact energy and decrease the deceleration of the occupant inside. In addition, low peak load will yield low decelerations and this is one of the key points that should be controlled during vehicle passive safety component design. In this regard, pultruded bumper beam shows a maximum deformation with a minimum mean crash load and an almost constant force diagram whose value is close to the maximum peak load. Thus this solution is giving a good interpretation of the ideal energy absorber. The reason behind is that pultruded composite products have fibers only in one direction, along the longitudinal direction in this particular case, therefore, when the beam is submitted to transverse loading, the composite material is relatively weak in the beam transverse direction and diffuse fractures take place at the extremities leading to a progressive failure. Therefore, as far as it is possible to control the displacement or keeping the displacement within the design limit, besides the previously mentioned mechanical and physical properties, this progressive deformability is an important feature in the passive safety behavior of the bumper component.

## 5. Conclusions

The work is dedicated to the development of pultruded composite car bumper beam with the aim to maintain or improve its mechanical properties and energy absorption capability with respect to the metallic beam that is the reference normal production solution. The material change is aimed to mass reduction.

Pultrusion technology has been chosen for its interesting features that fit quite well with the typical geometrical configuration of the considered application.

While designing this composite solution of the bumper transverse beam, design optimization process has been adopted, by considering as design variables both the shape to the beam cross section, the wall thickness in the optimized section and the beam curvature.

For this objective, numerical simulations have been conducted and structural results for the bumper beam have been compared between the new composite optimized solution and the normal production one. The following important conclusions can be drawn.

- For transversally loaded composite components like automotive bumper beam, properly optimized and located stress concentration zone or beam corners, can serve as crash triggering mechanism, to initiate cracks formation and to develop progressive tear along beam longitudinal axis. As the main portion of impact kinetic energy is absorbed through this longitudinal tearing, the number and location of folds need to be optimized.
- When the existing metallic vehicle bumper beam is substituted with composite beam, the beam curvature should be modified accordingly, because in composite bumper beam development, optimal choice of bumper beam curvature radius, besides improving vehicle aerodynamic and architecture, actually can give a relevant contribution to vehicle safety.
- Finally, material comparison study shows that E-Glass pultruded bumper beam has comparable energy absorption with steel and E-Glass fabric but has better progressive failure mode with reduced peak load. Therefore, introducing pultruded composite products as a safety component in automotive industries, besides manufacturing benefits, does improve vehicle safety.

## Acknowledgements

Authors would like to acknowledge the valuable contributions from Dr. Brunetto Martorana from FIAT Research Center, who shared his special knowledge about composite materials through technical discussions and gave us several suggestions.

Authors would like as well to acknowledge that part of the research activity, whose main results are presented in this paper, has been conducted within the frame of the research project “MACADI” (DM 60703) granted to IMAST S.c.a.r.l. and funded by the M.I.U.R.

## References

- [1] Campbell FC. Manufacturing processes for advanced composites. Elsevier; 2004.
- [2] Milwich M. Thermoplastic braid pultrusion. In: Proc. ICCM17 – XVII Int. conf. composite materials, Edinburgh (UK), 27–31 July, 2009.
- [3] Jimenez A, Miravete A, Larrode E, Revuelta D. Effect of trigger geometry on energy absorption in composite profiles. *Compos Struct* 2004;48:107–11.
- [4] Charoenphan Saiphon, Bank Lawrence C, Plesha Michael E. Progressive tearing failure in pultruded composite material tubes. *Composite Structures* 2004;63: 45–52.
- [5] Kim KJ, Won ST. Effect of structural variables on automotive body bumper impact beams. *Int J Automot Technol* 2008;9(6):713–7.
- [6] Boria S, Belingardi G. Numerical investigation of energy absorbers in composite materials for automotive applications. *Int J Crashworthiness* 2012;17(4):345–56. <http://dx.doi.org/10.1080/13588265.2011.648516>.
- [7] Suranaree J. Study on impact responses of pultruded GFRP, steel and aluminium beams by using drop weight impact test. *Sci Technol* 2008;15(3).



- [8] Palmer W, Bank LC, Gentry TR. – Progressive tearing failure of pultruded composite box beams: experiment and simulation. *Compos Sci and Technol* 1998;58(8):1353–13359.
- [9] Davoodi MM, Sapuan SM, Ahmad D, Aidy Khalina A, Jonoobi M. Concept selection of car bumper beam with developed hybrid bio-composite material. *Mater Des* 2011;32:4857–65.
- [10] Hirao NT, Kotera K, Nakamae M, Inagaki K, Kenafm H. Reinforced biodegradable composite. *Compos Sci Technol* 2003;63(9):1281–6.
- [11] Palanivelu S, Van Paepegem W, Degrieck J, Kakogiannis D, Van Ackeren J, Van Hemelrijck D, et al. Parametric study of crushing parameters and failure patterns of pultruded composite tubes using cohesive elements and seam, Part I: Central delamination and triggering modelling. *Polym Test* 2010;29:729–41.
- [12] Tabiei A, Svenson A, Hargarvec M, Bankd L. Impact performance of pultruded beams for highway safety applications. *Compos Struct* 1998;42:231–7.